

## Ab Initio Molecular Dynamics Simulations of Elimination Reactions in Water Solution: Exploring the Borderline Region between the E1cb and E2 Reaction Mechanisms

Filippo De Angelis,<sup>\*,†</sup> Francesco Tarantelli,<sup>†,‡</sup> and Sergio Alunni<sup>‡</sup>

Istituto CNR di Scienze e Tecnologie Molecolari (ISTM), c/o Dipartimento di Chimica, Università di Perugia, Via elce di Sotto 8, I-06213, Perugia, Italy, and Dipartimento di Chimica, Università di Perugia, Via Elce di Sotto 8, I-06213, Perugia, Italy

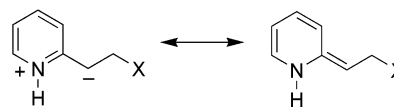
Received: March 2, 2006; In Final Form: April 13, 2006

We report a theoretical study, based on ab initio molecular dynamics simulations in water solution, of the mechanism of base-induced  $\beta$ -elimination reactions in systems activated by the pyridyl ring, with halogen leaving groups. The systems investigated represent borderline cases, where it is uncertain whether the reaction proceeds via a carbanion intermediate (E1cb,  $A_{\text{xh}}D_{\text{H}} + D_{\text{N}}$ ) or via the concerted loss of a proton and the halide (E2,  $A_{\text{N}}D_{\text{E}}D_{\text{N}}$ ) upon base attack. Recent theoretical and experimental evidence points toward the lack of a net distinction between the E1cb and E2 reaction paths, which seem to merge smoothly into each other in these borderline cases (Alunni, S.; De Angelis, F.; Ottavi, L.; Papavasileiou, M.; Tarantelli, F. *J. Am. Chem. Soc.* **2005**, *127*, 15151–15160). In this study, we explore the dynamics on the potential energy surface for the reaction of 2-(2-fluoroethyl)-1-methyl pyridinium with  $\text{OH}^-$  by means of Car–Parrinello simulations in water solution. Our results indicate that the reaction mechanism effectively evolves through the potential energy region of the carbanion: the carbon–fluoride bond breaks only after the carbon–hydrogen bond, confirming the conclusions of a recently reported study of the potential energy surface for this system.

### Introduction

Base-induced  $\beta$ -elimination reactions, with the formation of a carbon–carbon double bond, are fundamental chemical reactions and particularly important is the understanding of the mechanisms with which they take place with different substrates and in various solution environments. In particular, being able to distinguish between concerted and stepwise mechanisms is a very relevant issue both in chemistry<sup>1–13</sup> and in biochemistry.<sup>14</sup> The nature of the borderline region between concerted and stepwise mechanisms is yet unclear,<sup>5,15</sup> and an important aspect of this problem is establishing whether there is smooth continuity or distinct discontinuity between the E2 concerted and the E1cb stepwise mechanisms. The distinction between the E2 ( $A_{\text{xh}}D_{\text{H}}D_{\text{N}}$ ) and the E1cb irreversible mechanism ( $A_{\text{xh}}D_{\text{H}}^* + D_{\text{N}}$ ) is a difficult task.<sup>1,5,15</sup> In fact, while diagnosis of the E1cb reversible mechanism ( $A_{\text{xh}}D_{\text{H}} + D_{\text{N}}^*$ ) can be made<sup>1</sup> by the presence of H/D exchange,<sup>16</sup> by studies of acid–base catalysis,<sup>16</sup> and by the inverse solvent isotope effect,<sup>16b,17</sup> the E2 mechanism characteristics are similar to those of an E1cb irreversible mechanism. In previous studies<sup>16a,17–20</sup> of  $\beta$ -elimination reactions in systems activated by the pyridine ring, we have determined a high value of the proton activating factor, PAF, defined as the ratio of the second-order rate constant for the nitrogen protonated substrate,  $\text{NH}^+$ , and that for the unprotonated substrate, N. With the 2-(2-fluoroethyl)pyridine substrate,<sup>19</sup> a PAF of  $3.6 \times 10^5$  was found (acetohydroxamate base, 50 °C,  $\mu = 1 \text{ M KCl}$ ) whereas with *N*-[2-(2-pyridyl)ethyl]quinuclidinium the PAF is  $5.2 \times 10^6$ . The high values of PAF observed were interpreted in terms of an E1cb mechanism and a strongly resonance-stabilized intermediate carbanion; see Scheme 1.

### SCHEME 1



Methylation<sup>19,20</sup> of the N atom of the pyridine ring provides also a high activation factor, similar to the one for protonation. However, several uncertainties remain about the  $\beta$ -elimination in these borderline systems.

Theoretical studies on  $\beta$ -elimination reactions have mainly focused on prototype substrates (mostly  $\text{CH}_3\text{CH}_2\text{X}$ , with X = halogen) and were generally limited to the gas phase.<sup>21–25</sup> Among the many different theoretical studies, of particular relevance is the series performed by Gronert,<sup>21</sup> Saunders,<sup>23</sup> and Jensen<sup>24</sup> using mainly ab initio (MP2–MP4) calculations. It is also worth mentioning the study by Bickelhaupt et al.,<sup>22</sup> who performed a two-dimensional scan of the potential energy surface for the  $\text{CH}_3\text{CH}_2\text{F}$  substrate using density functional theory (DFT) calculations. More recently, the  $\text{CH}_3\text{CH}_2\text{F}$  substrate has been the subject of ab initio molecular dynamics simulations in the gas phase,<sup>25</sup> aimed at providing a detailed description of the free-energy landscape for the competing elimination/substitution reactions.

We have recently reported a combined experimental and theoretical study,<sup>26</sup> based on DFT calculations in solution, of the borderline region between E1cb and E2 reaction mechanisms in systems activated by the pyridine ring. In particular, we investigated 2-(2-fluoroethyl)pyridine and its chlorine and bromine analogues, with and without methyl activation at the nitrogen. There are several biological processes where the stabilization of a carbanion by the quaternized nitrogen of a heteroaromatic group plays an important role,<sup>14,27</sup> so the study of such prototype systems is very important.

\* To whom correspondence should be addressed. E-mail: filippo@thch.unipg.it.

<sup>†</sup> Istituto CNR di Scienze e Tecnologie Molecolari, Università di Perugia.

<sup>‡</sup> Dipartimento di Chimica, Università di Perugia.

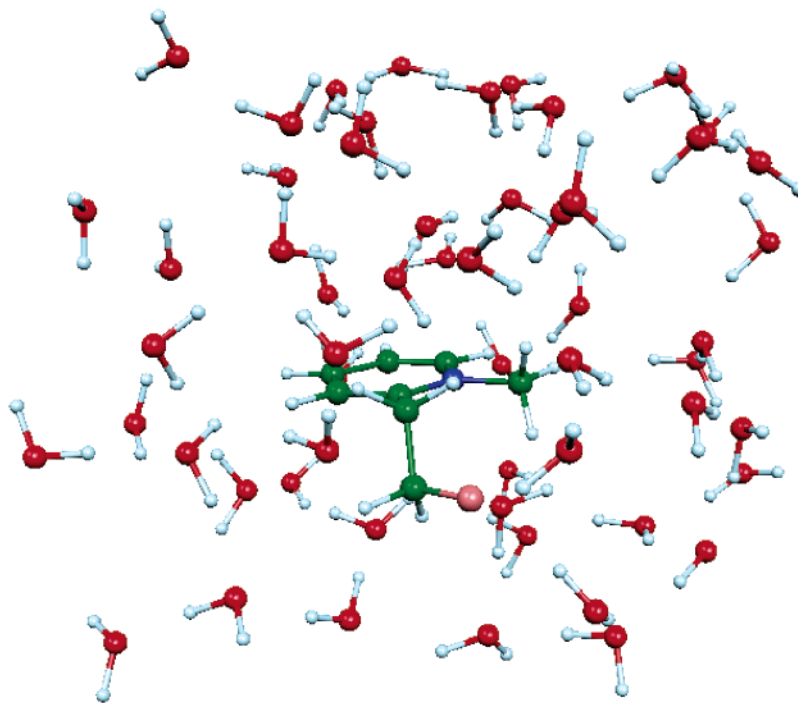


**Figure 1.** Molecular structure of the 2-(2-fluoroethyl)-1-methyl pyridinium reagent solvated by 56 water molecules.

By combining theoretical and experimental evidence, we have assigned an E2 mechanism to reactions of the nonmethylated substrates, regardless of the halide leaving group, while for the methylated substrates a change from an E1cb to an E2 mechanism is observed upon going from F to heavier halide leaving groups.<sup>26</sup> In the same study, we characterized the bidimensional potential energy surface (PES) in solution for the reaction of 2-(2-fluoroethyl)-1-methyl pyridinium with  $\text{OH}^-$  and proposed a tentative reaction dynamics based on the characteristics of the PES.

To assess conclusively the validity of those results, we have now studied, by *ab initio* molecular dynamics simulations in water solution, the reaction of 2-(2-fluoroethyl)-1-methyl pyridinium with  $\text{OH}^-$ , by means of the Car–Parrinello method,<sup>28</sup> obtaining hitherto inaccessible details of the reaction dynamics in this borderline system. We report the results in the present paper, showing that the reaction takes place passing through the region on the PES corresponding to the carbanion: the  $\text{C}_2\text{—F}$  bond breaks only after the  $\text{C}_1\text{—H}$  bond has been considerably elongated, leading to the olefin product. The main difference with our previous calculations is that in ref 26 we performed static geometry optimizations, incorporating a few water molecules in our model and describing the residual solvation effects by means of a polarizable continuum model, while in the present investigation we explicitly include 55 water molecules in our quantum mechanical calculations and sample the reactive PES by means of *ab initio* molecular dynamics simulations.

### Model and Computational Details

The optimized geometries of the reagent (R), carbanion (C), and olefin product (P) and the bidimensional PES have been previously calculated with the Gaussian 03 package<sup>29</sup> at the B3LYP/6-31++G\*\* level,<sup>30</sup> including solvation effects by means of the conductor-like polarizable continuum model (C-PCM),<sup>31</sup> as detailed in ref 26. We have shown that the present level of theory provides free-energy barriers and  $\text{pK}_a$  values in good agreement with experimental values.<sup>26</sup> We note that

solvation has a crucial effect in the reactions investigated: indeed, for the analogous nonmethylated reagent, both experimental evidence and B3LYP/6-31++G\*\* calculations in solution point to the lack of a stable carbanion, while a local minimum corresponding to a carbanion intermediate is found *in vacuo*.<sup>26</sup>

*Ab initio* molecular dynamics simulations (AIMD) were performed on the system composed of 2-(2-fluoroethyl)-1-methyl pyridinium and  $\text{OH}^-$ , solvated by 55 water molecules; see Figure 1. The number of water molecules was obtained considering the same simulation cell employed for a 64 waters simulation at the density of  $1 \text{ g/cm}^3$ ,<sup>32</sup> and subtracting the number of water molecules corresponding to the volume of the solvation cavity obtained from C-PCM calculations on the reagent. For AIMD simulations, we used the parallel version<sup>33</sup> of the Car–Parrinello (CP) code implementing Vanderbilt pseudopotentials.<sup>34</sup> The PBE exchange–correlation<sup>35</sup> functional was used. The Kohn–Sham orbitals (density) were expanded in plane waves up to an energy cutoff of 25 (200) Ry. Periodic boundary conditions were used by placing the system in a cubic box of  $12.4 \text{ \AA}$ . The equations of motion were integrated using a time step of 5 au (0.121 fs) with an electronic fictitious mass  $\mu = 500 \text{ au}$ . Constrained CP simulations were performed by means of the SHAKE algorithm,<sup>36</sup> employing the slow-growth method,<sup>37</sup> in which the constrained parameter is slowly varied as a function of the simulation time in such a way that the PES along the considered constraint is dynamically sampled. To maintain the system in thermal equilibrium, a Nosé thermostat,<sup>38</sup> which creates a canonical (NVT) ensemble, was applied to both nuclear and electronic degrees of freedom. A point which needs to be stressed here is that we only mean to exploit the exploratory power of AIMD simulations, without performing any thermodynamical integration along the selected reaction coordinate. This procedure, which could in principle lead to the free-energy variation along the reaction path, would require much longer simulation times than the ones used here to provide free-energy estimates.

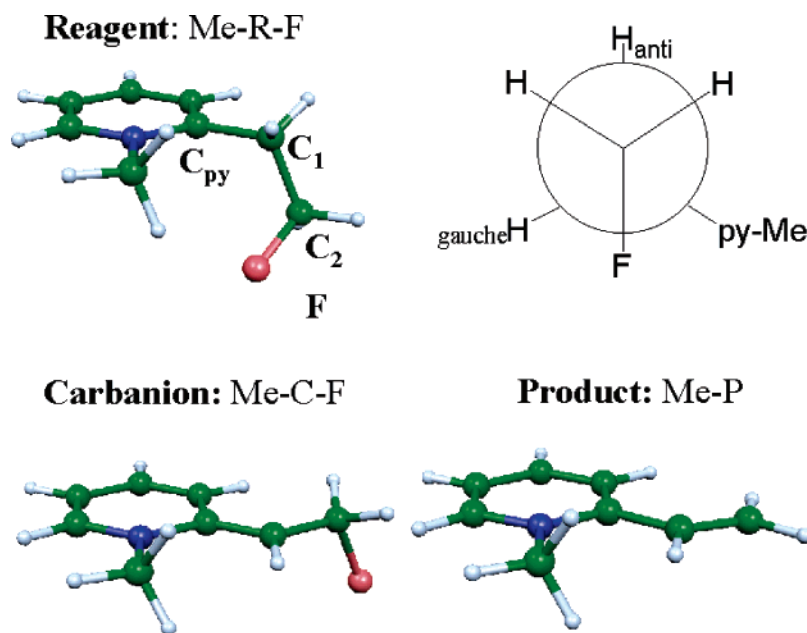


**Figure 2.** Optimized molecular structures of the 2-(2-fluoroethyl)-1-methyl pyridinium reagent (R), carbanion (C), and olefin product (P). Also shown is a Newman projection of the reagent.

## Result and Discussion

The optimized molecular structures<sup>26</sup> of the methylated reagent, carbanion, and product are displayed in Figure 2. The calculated  $C_{py}-C_1$  and  $C_1-C_2$  distances show values close to typical single carbon-carbon bonds in the reagent, while in the carbanion a considerable shortening of both parameters takes place, reflecting a high degree of conjugation involving these two carbon-carbon bonds. On the contrary, the  $C_2-F$  bond length in the carbanion is elongated with respect to the reagent (1.498 vs 1.415 Å, respectively), indicating the weakening of the  $C_2-F$  bond which precedes the loss of the halogen leaving group. We notice that this elongation of the  $C_2-F$  bond (0.083 Å) is comparable with those observed in a previous study of fluorinated carbanions, where such differences were shown to have a sizable effect on the fluorine isotope effects and contributed to the stabilization of carbanion intermediates by the so-called negative ion hyperconjugation.<sup>23b</sup> When going from the reagent to the carbanion, a clear change from an  $sp^3$  to an  $sp^2$  hybridization of the  $C_1$  carbon is observed, as testified by the change in the  $\angle N-C_{py}-C_1-C_2$  dihedral angle from 89.7 to 178.4°, with the latter value corresponding to an almost perfect planar structure. The geometrical parameters of the carbanion are therefore consistent with the enamine structure displayed as the right-hand resonance contributor in Scheme 1. For the olefin product, an inversion of the  $C_{py}-C_1$  and  $C_1-C_2$  distances takes place with respect to the carbanion and the  $C_1-C_2$  distance (1.341 Å) is close to (only slightly larger than) typical double carbon-carbon bond distances. Similar to the carbanion, a planar structure is calculated for the olefin product. Comparison of geometrical parameters calculated in vacuo and in solution for the reagent and carbanion shows that solvation weakens the  $C_2-F$  bond: shorter C-F distances are calculated in vacuo than in solution (1.392 and 1.444 Å vs 1.415 and 1.498 Å for the reagent and carbanion, respectively). This is expected since the solvent polarity stabilizes the negative charge on the F atom.

**Reaction Mechanism.** To provide a detailed description of the  $\beta$ -elimination reaction mechanism, we performed constrained AIMD simulations. In doing so, an approximate reaction coordinate (RC) had to be selected. Obviously, the choice of a suitable approximate RC is crucial for the proper description

of the reaction mechanism and, in the present case, a natural and adequate procedure appears that of sampling the PES along the distance of approach of the base to the substrate, since the base has to attack the reagent to abstract a proton. We have therefore chosen the distance between the oxygen of the  $OH^-$  and the  $C_1-H$  hydrogen, since this choice does not introduce any explicit constraint on the  $C_1-H$  and  $C_2-F$  bond distances, whose manner of variation, concerted or stepwise, upon approach of the base, fundamentally characterizes the reaction mechanism. By shortening the approximate RC, we simulate the base approach to the substrate, which should eventually lead to the proton abstraction from the substrate and the concomitant formation of a water molecule and the carbanion intermediate and/or the olefin product. In ref 26, we have shown that this approximate RC effectively describes the reaction evolution.

We first performed a 2.0 ps AIMD simulation of the reagent solvated by 56 water molecules at a temperature of 300 K. After this, we selected a water molecule close to the  $C_1-H$  hydrogen and replaced it by  $OH^-$ . We then thermalized the resulting system for 0.7 ps to a temperature of at 300 K maintaining an RC value of 2.5 Å, roughly corresponding to a noninteracting or weakly interacting base and substrate. After this time, the selected RC was reduced in about 3.0 ps to 0.95 Å, roughly corresponding to the H-OH bond length in a water molecule.

A first important insight into the reaction dynamics can be gained by analyzing the evolution of the  $C_1-H$  and  $C_2-F$  distances as a function of the simulation time (or approximate RC value). The parameters considered are both expected to increase considerably from their equilibrium values in the reagent upon formation of the olefin product, reflecting the proton abstraction by the base and the eventual breaking of the  $C_2-F$  bond. The  $C_1-H$  and  $C_2-F$  distances are plotted as a function of the simulation time in Figure 3, which clearly shows that the elimination reaction effectively takes place after 3.0 ps of simulation, that is, after the  $OH^-$  base has approached the substrate to a distance of about 1.3 Å.

Indeed, starting at 2.0 ps, the  $C_1-H$  bond begins slightly to increase in length and, after 3.0 ps, it breaks up to 3.5 Å, testifying to proton abstraction by the base. Notably, the calculated transition state geometry for the elimination reaction,

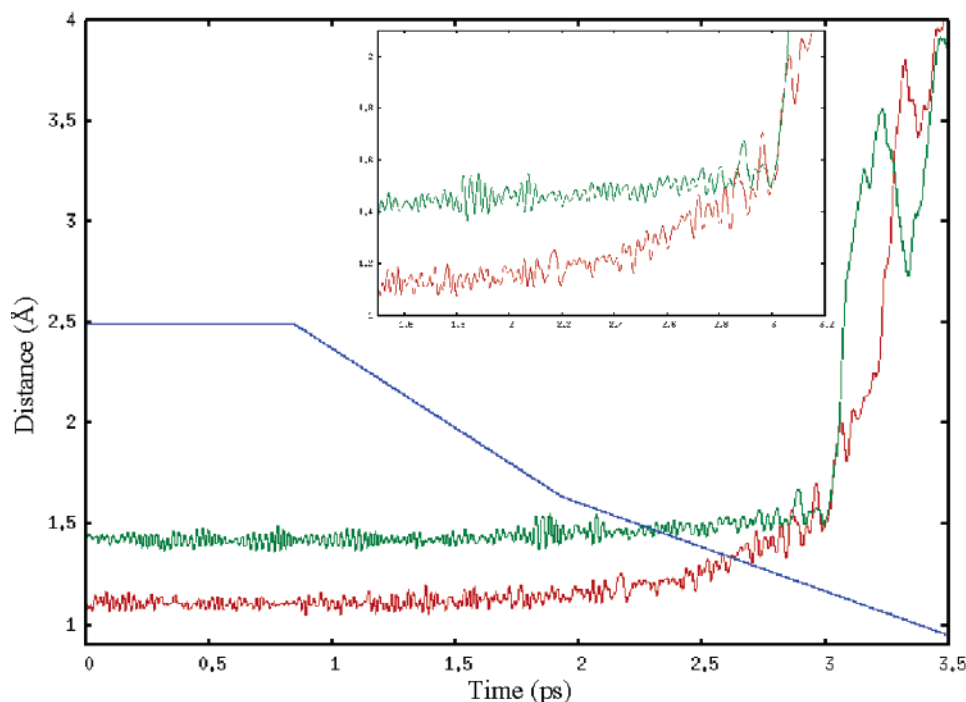


**Figure 3.** Time evolution of the distances  $C_1-H$  (red line),  $C_2-F$  (green line), and approximate RC (blue line). Inset: detail of the time span 1.5–3.2 ps.

characterized by an approximate RC value of  $1.26 \text{ \AA}$ ,<sup>26</sup> is consistent with the results of the present dynamics simulation. Indeed, this RC value corresponds to a simulation time of about 3.0 ps, when the sudden increase in the  $C_1-H$  distance is observed.

Most interestingly, our simulation shows that the  $C_2-F$  distance remains close to the equilibrium value it has in the reagent up to 2.5 ps and it increases slightly over the next 0.5 ps, reflecting the elongation of this parameter which is calculated upon going from the reagent to the carbanion minima; see above. After 3.0 ps, the  $C_2-F$  bond suddenly breaks, reflecting the elimination of the fluoride leaving group. As can be noticed from Figure 3, only after the  $C_1-H$  distance has exceeded  $1.5 \text{ \AA}$  does the  $C_2-F$  bond begin to dissociate.

Further insight into the reaction dynamics can be gained by analyzing the time evolution of the  $\angle N-C_{py}-C_1-C_2$  dihedral angle. This parameter assumes values close to about  $90^\circ$  in the reagent, while a value close to  $180^\circ$  characterizes the planar structures of the carbanion and of the olefin product. The time evolution of the  $\angle N-C_{py}-C_1-C_2$  dihedral angle is reported in Figure 4, which shows that this parameter oscillates about  $100^\circ$ , characterizing the reagent, up to 2.0 ps. After this time, this dihedral angle steadily increases to  $160^\circ$  within 3.0 ps. Later, due to the sudden breaking of the  $C_2-F$  bond, it performs some broad oscillations.

By combining the information of Figures 3 and 4, we can conclude that a configuration close to that of the carbanion intermediate is effectively accessed in the time slice from 2.5 to 3.0 ps, with the latter time corresponding to breaking of the  $C_2-F$  bond. During this time interval, the  $C_1-H$  bond is breaking while the  $C_2-F$  bond is not yet broken.

The emerging picture is perfectly in line with our previous calculations, which showed only a modest energy barrier for fluoride loss from the carbanion. This is consistent with the fact that the carbanion is observed only as a short-lived transient species in our AIMD simulation. The details of the reactive PES together with optimized transition state structures for the  $C_1-H$  and  $C_2-F$  bond breaking are illustrated in Figure 5.

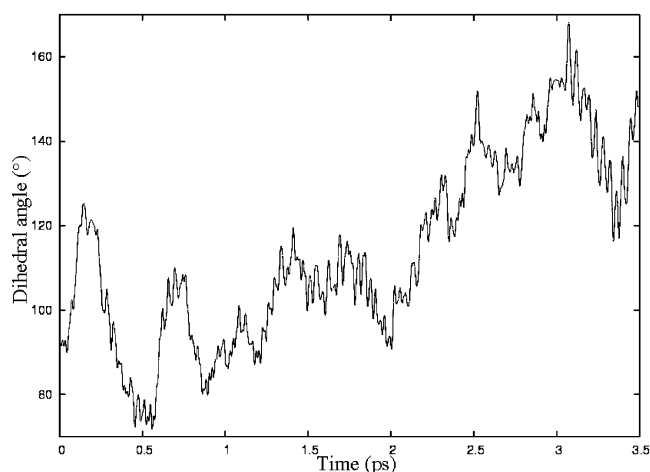


**Figure 4.** Time evolution of the  $\angle N-C_{py}-C_1-C_2$  dihedral angle during the elimination reaction.

It appears that the barrier to halide expulsion is initially (for short values of the  $C_1-H$  distance) very high but drops progressively to almost zero for  $C_1-H$  values larger than  $1.5\text{--}1.8 \text{ \AA}$ . At this stage of the reaction, the calculated PES is almost flat, so that the system can access the region around the carbanion and proceed easily toward the olefin product. We note that transition states corresponding to  $C_1-H$  and  $C_2-F$  bond breaking have been calculated on the bidimensional PES for  $C_1-H$  and  $C_2-F$  values of  $1.259$  and  $1.474 \text{ \AA}$ , respectively, and for a  $C_2-F$  value of  $1.750 \text{ \AA}$ . In addition to the static information provided by the calculated PES and transition states, our AIMD simulations allow us to define in detail the relative timing of the  $C_1-H$  and  $C_2-F$  bond breaking. We incidentally remark that the transition state structure for the  $C_1-H$  bond breaking calculated in vacuo is different from that calculated in solution, with  $C_1-H$  and  $C_2-F$  distances of  $1.353$  and  $1.468 \text{ \AA}$ , respectively.

**Stereochemistry of the Base Attack.** It is finally very interesting to analyze in detail the stereochemistry of the base



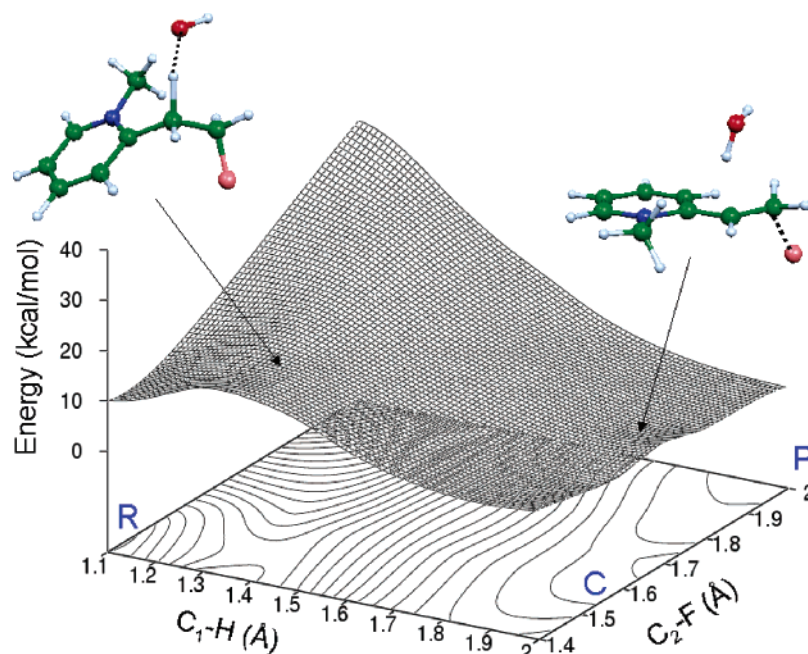


**Figure 5.** 3D plot and contour plot of the computed potential energy surface for the elimination reaction, as a function of the  $C_1-H$  and  $C_2-F$  (Å) bond distances. Optimized structures of the transition states for the  $C_1-H$  and  $C_2-F$  bond breaking are also reported.<sup>26</sup>

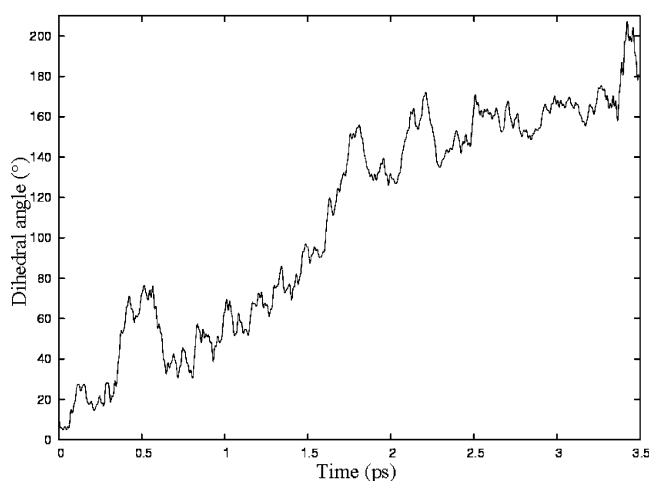


**Figure 6.** Time evolution of the  $\angle H-C_1-C_2-F$  dihedral angle during the elimination reaction.

approach to the substrate. We previously found that a base attack to the  $C_1$ -bound proton anti to the fluoride leaving group features a slightly lower (1.8 kcal/mol) energy barrier than that for the gauche attack.<sup>26</sup> To check whether the anti attack is really favored, we started the AIMD simulation with the base attacking the syn hydrogen and allowed the system to fully dynamically relax during the simulation. The stereochemical evolution of the reaction can be followed by analyzing the time evolution of the  $\angle H-C_1-C_2-F$  dihedral angle, where the  $C_1$ -bound hydrogen atom is the one undergoing the attack. This angle assumes values close to 0, 60, and 180° for the syn, gauche, and anti conformations, respectively, and its time evolution is reported in Figure 6.

As can be noticed, the  $\angle H-C_1-C_2-F$  dihedral angle is initially close to the value corresponding to a syn configuration and reaches values typical of the gauche configuration, corresponding to the equilibrium structure of Figure 2, within 0.5 ps. As the reaction proceeds, however, this parameter increases continuously, to exceed 150° after 2.0 ps, reflecting the change from the syn to the anti configuration which accompanies the reaction, which effectively takes place at the expenses of the

$C_1$ -bound hydrogen atom. The preferential anti attack might be explained considering that this configuration minimizes the electrostatic repulsion between the incoming  $OH^-$  base and the partially negatively charged fluorine substituent, which eventually leaves the substrate as  $F^-$ . We finally notice that the carbanion intermediate and olefin product might assume E or Z conformations and that in our AIMD simulations the Z conformer of these species is formed.

## Conclusions

We have studied the mechanism of the elimination reaction of 2-(2-fluoroethyl)-1-methyl pyridinium in  $OH^-/H_2O$ . In particular, we have explored, by Car-Parrinello molecular dynamics in water solution, the time evolution of the elimination reaction to understand the details of its reaction mechanism and compared these results with those already obtained for the relevant ab initio multidimensional potential energy surface. The process studied, a prototype of elimination reactions in systems activated by the pyridine ring, is known from both experimental and theoretical data to represent an interesting case of the borderline region between the E1cb and E2 reaction mechanisms.<sup>26</sup> The PES in solution is characterized by an energy barrier to fluoride loss which decreases rapidly when the  $C_1-H$  bond lengthens upon the proton-abstracting base attack, so that the carbanion is a relatively short-lived species. The dynamical simulation shows indeed that the reaction proceeds via an E1cb mechanism where the base attack causes a progressive significant stretching of the  $C_1-H$  bond from about 1 Å to more than 1.5 Å over a time scale of about 3 ps, during which time the  $C_2-F$  bond remains essentially at the equilibrium value of the reagent. After about 3 ps, the breaking of the  $C_1-H$  bond accelerates and is essentially complete in the next 0.2 ps, but during this time, the  $C_2-F$  suddenly breaks too, leading almost instantaneously to the formation of the olefin product. This picture is in agreement with the previously reported mechanistic description of a relatively flat region of the PES corresponding to a carbanionic metastable intermediate.

Both the ab initio calculation of the reaction energetics and the dynamical simulation evidence the absolute need to account

for the solvent environment to describe these reactions reliably. The CP dynamics also accounts accurately for a very interesting aspect of the stereochemistry of the elimination reaction, namely, the preference for base attack to the proton in an anti position to the fluoride substituent: starting the simulation with the base approaching the syn-positioned proton leads to a progressive rotation of the system about the C<sub>1</sub>–C<sub>2</sub> bond toward the favored anti configuration before the proton is abstracted from the substrate.

Our work shows that the effective combination of advanced experimental investigations and state-of-the-art computational simulation of the energetics and dynamics of elimination reactions permits to cast light on yet uncertain aspects of this all-important chemistry. Further work on this series of systems with different isomers and different leaving groups is in progress.

**Acknowledgment.** Thanks are due to the Italian Ministero dell'Istruzione, dell'Università e della Ricerca (MIUR) for financial support.

## References and Notes

- (1) (a) Saunders, W. H., Jr.; Cockerill, A. F. *Mechanism of Elimination Reaction*; Wiley-Interscience Publication: New York, 1973; Vol. II, pp 60–68. (b) Baciocchi, E. *The Chemistry of Halides, Pseudo Halides and Azides*, supplement D; Patai, S., Rappoport, Z., Eds.; Wiley: Chichester, U.K., 1983. (c) Gandler, J. R. *The Chemistry of Double Bonded Functional Group*; Patai, S., Ed.; Wiley: Chichester, U.K., 1989. (d) Saunders, W. H., Jr. *Acc. Chem. Res.* **1976**, 9, 19. (e) Stirling, C. J. M. *Acc. Chem. Res.* **1979**, 12, 198. (f) Cavestri, R. C.; Fedor, L. R. *J. Am. Chem. Soc.* **1970**, 92, 4610. (g) Fedor, L. R.; Glave, W. R. *J. Am. Chem. Soc.* **1971**, 93, 985.
- (2) (a) Gandler, J. R.; Storer, W. J.; Ohlberg, D. A. *J. Am. Chem. Soc.* **1990**, 112, 7756. (b) Gandler, J. R.; Yokoyama, T. *J. Am. Chem. Soc.* **1984**, 106, 130.
- (3) Gandler, J. R.; Jencks, W. P. *J. Am. Chem. Soc.* **1982**, 104, 1937.
- (4) (a) Thibblin, A. *J. Am. Chem. Soc.* **1989**, 111, 5412. (b) Quingshui, M.; Thibblin, A. *J. Am. Chem. Soc.* **1995**, 117, 1839. (c) Quingshui, M.; Thibblin, A. *J. Am. Chem. Soc.* **1995**, 117, 9399.
- (5) (a) More O'Ferrall, R. A.; Warren, P. J. *J. Chem. Soc., Chem. Commun.* **1975**, 483. (b) More O'Ferrall, R. A.; Warren, P. J.; Ward, P. M. *Acta Univ. Uppsol., Symp. Univ. Uppsol.* **1978**, 12, 209.
- (6) More O'Ferrall, R. A.; Larkin, F.; Walsh, P. *J. Chem. Soc., Perkin Trans. 2* **1982**, 1573.
- (7) Larkin, F.; More O'Ferrall, R. A. *Aust. J. Chem.* **1983**, 36, 1831.
- (8) Thibblin, A. *J. Am. Chem. Soc.* **1988**, 110, 4582.
- (9) Ölwegård, M.; McEwen, I.; Thibblin, A.; Ahlberg, P. *J. Am. Chem. Soc.* **1985**, 107, 7494.
- (10) Jencks, W. P. *Chem. Soc. Rev.* **1981**, 10, 345.
- (11) Marshall, D. R.; Thomas, P. J.; Stirling, C. J. M. *J. Chem. Soc., Perkin Trans. 2* **1977**, 1914.
- (12) Banait, N. S.; Jencks, W. P. *J. Am. Chem. Soc.* **1990**, 112, 6950.
- (13) (a) Thibblin, A. *Chem. Soc. Rev.* **1993**, 427. (b) Jencks, W. P. *Acc. Chem. Res.* **1980**, 161. (c) Cho, B. R.; Kim, Y. K.; Yoon, P.-O. M. *J. Am. Chem. Soc.* **1997**, 119, 691. (d) Koch, H. F.; Lodder, G.; Koch, J. G.; Bogdon, D. J.; Brown, G. H.; Carlson, C. A.; Dean, A. B.; Hage, R.; Han, P.; Hopman, J. C. P.; James, L. A.; Knappe, P. M.; Roos, E. C.; Sardina, M. L.; Dawyer, R. A.; Scott, B. O.; Testa, C. A., III; Wickham, S. D. *J. Am. Chem. Soc.* **1997**, 119, 9965. (e) Koch, H. F.; McLennan, D. J.; Koch, J. G.; Tumas, W.; Dobson, B.; Koch, N. H. *J. Am. Chem. Soc.* **1983**, 105, 1930. (f) Koch, H. F.; Koch, J. G.; Koch, N. H.; Koch, A. S. *J. Am. Chem. Soc.* **1983**, 105, 2388.
- (14) (a) Abeles, R. H.; Frey, P. A.; Jencks, W. P. *Biochemistry*; Jones and Bartlett Publisher: Boston, MA, 1992. (b) Voet, D.; Voet, J. G. *Biochemistry*; John Wiley & Sons: New York, 1990.
- (15) Larkin, F. G.; More O'Ferrall, R. A.; Murphy, D. G. *Collect. Czech. Chem. Commun.* **1999**, 64, 1833.
- (16) (a) Alunni, S.; Conti, A.; Palmizio Errico, R. *J. Chem. Soc., Perkin Trans. 2* **2000**, 453. (b) Keeffe, J. R.; Jencks, W. P. *J. Am. Chem. Soc.* **1983**, 105, 265.
- (17) Alunni, S.; Conti, A.; Palmizio Errico, R. *Res. Chem. Intermed.* **2001**, 27, 653.
- (18) Alunni, S.; Busti, A. *J. Chem. Soc., Perkin Trans. 2* **2001**, 778.
- (19) Alunni, S.; Laureti, V.; Ottavi, L.; Ruzziconi, R. *J. Org. Chem.* **2003**, 68, 718.
- (20) Alunni, S.; Ottavi, L. *J. Org. Chem.* **2004**, 69, 2272.
- (21) (a) Gronert, S. *J. Am. Chem. Soc.* **1991**, 113, 6041. (b) Gronert, S. *J. Am. Chem. Soc.* **1992**, 114, 2349. (c) Gronert, S. *J. Am. Chem. Soc.* **1993**, 115, 652. (d) Gronert, S.; Merrill, G. N.; Kass, S. R. *J. Org. Chem.* **1995**, 60, 488. (e) Gronert, S.; Freed, P. *J. Org. Chem.* **1996**, 61, 9430. (f) Gronert, S.; Kass, S. R. *J. Org. Chem.* **1997**, 62, 7991. (g) Merrill, G. N.; Gronert, S.; Kass, S. R. *J. Phys. Chem. A* **1997**, 101, 208.
- (22) Bicklehaupt, F. M.; Baerends, E. J.; Nibbering, N. M. M.; Ziegler, T. *J. Am. Chem. Soc.* **1993**, 115, 9160.
- (23) (a) Saunders, W. H., Jr. *J. Org. Chem.* **1997**, 62, 244. (b) Saunders, W. H., Jr. *J. Org. Chem.* **1999**, 64, 861. (c) Saunders, W. H., Jr. *J. Org. Chem.* **2000**, 65, 681.
- (24) (a) Glad, S. S.; Jensen, F. *J. Am. Chem. Soc.* **1994**, 116, 9302. (b) Glad, S. S.; Jensen, F. *J. Phys. Chem.* **1996**, 100, 16892. (c) Glad, S. S.; Jensen, F. *J. Phys. Chem.* **1997**, 62, 2253.
- (25) (a) Mugnai, M.; Cardini, M.; Schettino, V. *J. Phys. Chem. A* **2003**, 2540. (b) Ensing, B.; Laio, A.; Gervasio, F. L.; Parrinello, M.; Klein, M. L. *J. Am. Chem. Soc.* **2004**, 126, 9492. (c) Ensing, B.; Klein, M. L. *Proc. Natl. Acad. Sci.* **2005**, 102, 6755.
- (26) Alunni, S.; De Angelis, F.; Ottavi, L.; Papavasileiou, M.; Tarantelli, F. *J. Am. Chem. Soc.* **2005**, 127, 15151.
- (27) *Angew. Chem., Int. Ed. Engl.* **1995**, 34, 1464.
- (28) Altson, W. C.; Haley, K.; Kanski, R.; Murray, C. J.; Pranata, J. *J. Am. Chem. Soc.* **1996**, 118, 6562.
- (29) Car, R.; Parrinello, M. *Phys. Rev. Lett.* **1985**, 55, 2471.
- (30) Frisch, M. J.; Trucks, G. W.; Schlegel, H. B.; Scuseria, G. E.; Robb, M. A.; Cheeseman, J. R.; Montgomery, J. A., Jr.; Vreven, T.; Kudin, K. N.; Burant, J. C.; Millam, J. M.; Iyengar, S. S.; Tomasi, J.; Barone, V.; Mennucci, B.; Cossi, M.; Scalmani, G.; Rega, N.; Petersson, G. A.; Nakatsuji, H.; Hada, M.; Ehara, M.; Toyota, K.; Fukuda, R.; Hasegawa, J.; Ishida, M.; Nakajima, T.; Honda, Y.; Kitao, O.; Nakai, H.; Klene, M.; Li, X.; Knox, J. E.; Hratchian, H. P.; Cross, J. B.; Adamo, C.; Jaramillo, J.; Gomperts, R.; Stratmann, R. E.; Yazyev, O.; Austin, A. J.; Cammi, R.; Pomelli, C.; Ochterski, J. W.; Ayala, P. Y.; Morokuma, K.; Voth, G. A.; Salvador, P.; Dannenberg, J. J.; Zakrzewski, V. G.; Dapprich, S.; Daniels, A. D.; Strain, M. C.; Farkas, O.; Malick, D. K.; Rabuck, A. D.; Raghavachari, K.; Foresman, J. B.; Ortiz, J. V.; Cui, Q.; Baboul, A. G.; Clifford, S.; Cioslowski, J.; Stefanov, B. B.; Liu, G.; Liashenko, A.; Piskorz, P.; Komaromi, I.; Martin, R. L.; Fox, D. J.; Keith, T.; Al-Laham, M. A.; Peng, C. Y.; Nanayakkara, A.; Challacombe, M.; Gill, P. M. W.; Johnson, B.; Chen, W.; Wong, M. W.; Gonzalez, C.; Pople, J. A. *Gaussian 03*, revision B.04; Gaussian, Inc.: Pittsburgh, PA, 2003.
- (31) (a) Becke, A. D. *J. Chem. Phys.* **1993**, 98, 5648. (b) Ditchfield, R.; Hehre, W. J.; Pople, J. A. *J. Chem. Phys.* **1971**, 54, 724.
- (32) (a) Barone, V.; Cossi, M. *J. Phys. Chem. A* **1998**, 102, 1995. (b) Cossi, M.; Rega, N.; Scalmani, G.; Barone, V. *J. Comput. Chem.* **2003**, 24, 669.
- (33) Hetényi, B.; De Angelis, F.; Giannozzi, P.; Car, R. *J. Chem. Phys.* **2004**, 120, 8632.
- (34) Giannozzi, P.; De Angelis, F.; Car, R. *J. Chem. Phys.* **2004**, 120, 5903.
- (35) (a) Pasquarello, A.; Laasonen, K.; Car, R.; Lee, C.; Vanderbilt, D. *Phys. Rev. Lett.* **1992**, 69, 1982. (b) Pasquarello, A.; Laasonen, K.; Car, R.; Lee, C.; Vanderbilt, D. *Phys. Rev. B* **1993**, 47, 10142. (c) Vanderbilt, D. *Phys. Rev. B* **1990**, 41, 7892.
- (36) Perdew, J. P.; Burke, K.; Ernzerhof, M. *Phys. Rev. Lett.* **1996**, 77, 3865.
- (37) Ryckaert, J.-P.; Cicciotti, G.; Berendsen, H. J. C. *J. Comput. Phys.* **1977**, 23, 327.
- (38) Straatsma, T. P.; Berendsen, H. J. C.; Postma, J. P. M. *J. Chem. Phys.* **1986**, 85, 6720.
- (39) Nosé, S. *Mol. Phys.* **1984**, 52, 255.